

MIT Open Access Articles

Efficient CRISPR/Cas9-mediated genome editing in P. falciparum

The MIT Faculty has made this article openly available. **Please share** how this access benefits you. Your story matters.

Citation: Wagner, Jeffrey C, Randall J Platt, Stephen J Goldfless, Feng Zhang, and Jacquin C Niles. "Efficient CRISPR-Cas9-mediated Genome Editing in Plasmodium Falciparum." Nat Meth 11, no. 9 (August 10, 2014): 915–918.

As Published: <http://dx.doi.org/10.1038/nmeth.3063>

Publisher: Nature Publishing Group

Persistent URL: <http://hdl.handle.net/1721.1/99501>

Version: Author's final manuscript: final author's manuscript post peer review, without publisher's formatting or copy editing

Terms of use: Creative Commons Attribution-Noncommercial-Share Alike





Published in final edited form as:

Nat Methods. 2014 September ; 11(9): 915–918. doi:10.1038/nmeth.3063.

Efficient CRISPR/Cas9-mediated genome editing in *P. falciparum*

Jeffrey C. Wagner¹, Randall J. Platt^{1,2}, Stephen J. Goldfless¹, Feng Zhang^{1,2,3,4}, and Jacquin C. Niles¹

¹Department of Biological Engineering, Massachusetts Institute of Technology, Cambridge, Massachusetts, USA

²Broad Institute of MIT and Harvard, Cambridge, Massachusetts, USA

³McGovern Institute for Brain Research, Massachusetts Institute of Technology, Cambridge, Massachusetts, USA

⁴Department of Brain and Cognitive Sciences, Massachusetts Institute of Technology, Cambridge, Massachusetts, USA

Malaria is a major cause of global morbidity and mortality, and new strategies for treating and preventing this disease are needed. The protozoan parasite, *Plasmodium falciparum*, contributes to the annual 219 million cases and 655,000 deaths from malaria. Gene knockouts, while central to studying this parasite, are inefficient and present a substantial bottleneck. Here we show that the *Streptococcus pyogenes* Cas9 DNA endonuclease and single guide RNAs (sgRNAs) made *in situ* using T7 RNA polymerase (T7 RNAP) efficiently edit the *P. falciparum* genome. Targeting the native knob-associated histidine-rich protein (*kahrp*) and erythrocyte binding antigen 175 (*eba-175*) genes, we achieve high (50–100%) gene disruption frequencies within the usual timeframe for generating transgenic parasites. Our results demonstrate a straightforward strategy for efficiently manipulating the *P. falciparum* genome to facilitate basic biological studies, and drug and vaccine development efforts in a human pathogen of major significance to global health.

The most commonly used approach for modifying chromosomal loci in *P. falciparum* relies on spontaneous single- or double- crossover recombination using plasmids containing sequence homologous to the target region^{1–3}. This is extremely inefficient, and requires many months to achieve the desired outcome. Circular plasmids are used to transform *P. falciparum*, and these are preferentially maintained as episomes². Isolating rare parasites with the desired chromosomal integration event from a high episomally-transformed background requires protracted on/off selection drug cycling and/or negative selection procedures⁴, none of which increase the initial fraction of the population genetically modified as desired. Zinc finger nucleases (ZFNs) have recently been used to efficiently

Corresponding author: Jacquin C. Niles, jcniles@mit.edu.

Author Contributions

JCW generated all plasmid reagents, transgenic parasites and performed all experimental analyses of these lines. RJP performed *in vitro* Cas9 cleavage assays and deep sequencing. SJG collected SEM imaging data. JCW and JCN designed experiments and analyzed data. JCW and JCN wrote the manuscript with input from RJP and FZ. JCN supervised the research.

Competing Financial Interests

The authors declare no competing financial interests.

achieve targeted knockouts and allele replacements in *P. falciparum*⁵. However, each time a different genomic region is targeted, an intensive effort is required to develop and validate new sequence-specific nucleases that are not guaranteed to function effectively^{6,7}. Recently, efficient site-specific genome editing using Cas9 has been validated in several organisms^{8–12}. Here, a guide RNA (sgRNA) is used to direct Cas9 to a target site defined by a 5'-NGG-3' protospacer adjacent motif (PAM) and an upstream 20-nucleotide sequence selected based on Watson-Crick base pairing with the target site (Fig. 1a). These straightforward implementation rules make this a potentially versatile option for broadly accessible use in *P. falciparum*.

Implementing Cas9 RNA-guided nucleases in *P. falciparum* requires a validated strategy for producing sgRNAs *in situ*. While the strong *U6* promoter transcribed by the endogenous Pol III has been used to produce functional sgRNAs in other organisms^{9, 10, 12}, a functional *U6* promoter has not been defined in *P. falciparum*. Several *P. falciparum* Pol II promoters have been described. However, target transcripts produced from these promoters have long, heterogeneously sized 5' and 3' flanking regions^{13, 14}, and are likely produced at lower levels than Pol III-synthesized transcripts. Given this, we chose T7 RNA polymerase (T7 RNAP) for producing defined sgRNAs in *P. falciparum*, as it uses well-characterized promoter and terminator sequences to make transcripts of defined size and in high yield.

We first validated that functional T7 RNAP can be expressed in *P. falciparum*, as this had not previously been reported. We constructed a vector to express T7 RNAP (pT7 RNAP) using pfGNr (MRA-462; www.mr4.org) as a starting point (Fig. 1b). pT7 RNAP and pfGNr were separately transfected into 3D7 parasites and G418-selected episomal lines obtained. Western blot analysis confirmed that intact T7 RNAP is produced in the pT7 RNAP, but not the pfGNr transfected lines (Fig. 1c). To establish that the T7 RNAP produced is enzymatically active, we constructed several additional vectors (Fig. 1b). In pT7-RL1, the full-length *Renilla* luciferase (RL) coding sequence can be transcribed from a *T7* promoter-driven cassette as a reporter of *in situ* T7 RNAP activity. In the negative control pT7 RL2 and p T7 plasmids, the *T7* promoter and the entire *T7* expression cassette, respectively, have been deleted from pT7 RL1. We transfected 3D7 parasites with the various combinations shown in Figures 1d,e. Based on quantitative RT-PCR and Northern blot analyses, T7 RNAP made in the parasite is enzymatically active and, expectedly, produces target transcripts of the expected size only when a *T7* promoter is present. Importantly, T7 RNAP expression both in the absence and presence of a *T7* promoter driven expression cassette is well tolerated. No gross effects on parasite viability in the short term (Fig. 1f) or after prolonged periods of continuous culture (data not shown) were observed.

Guide RNAs produced *in vitro* using T7 RNAP and linearized plasmid DNA templates have been used to successfully induce Cas9-mediated editing in zebrafish and *Drosophila melanogaster*^{8, 11}. However, since *P. falciparum* maintains circular plasmids, a *T7* terminator is required to specify transcription termination. However, the *T7* terminator is mostly transcribed, and thus, sgRNAs produced from such templates will have the *T7* terminator-derived stem-loop region at their 3'-termini (sgRNA-T, Supplementary Fig. 1). As the impact of this additional sequence on sgRNA function was unknown, we first tested whether a sgRNA-T can direct specific cleavage of a DNA template *in vitro*. We PCR

amplified target DNA fragments from both the parasite *kahrp* and *eba-175* loci (nucleotides 619–2267 and 141–1363, respectively) containing predicted sgRNA target sites. We *in vitro* transcribed test *kahrp*- and *eba175*- sgRNA-Ts, and a control pUC19-sgRNA-T from circular plasmid templates. We then co-incubated Cas9-containing cell lysates, DNA templates and either test (*kahrp*- and *eba175*- sgRNA-T) or control (pUC19-sgRNA-T) to test cleavage activity. As shown in Supplementary Figure 1, both the *kahrp*- and *eba175*-sgRNA-Ts specifically and efficiently cleaved their respective target DNA, while the pUC19-sgRNA-T did not cleave the *kahrp* or *eba-175* templates. Thus, the additional sequence introduced when using the *T7* terminator does not interfere with Cas9 and sgRNA-T-mediated target cleavage *in vitro*.

Next, we determined whether sgRNA-T produced *in situ* can be used to successfully disrupt chromosomal loci in *P. falciparum*. We selected the *kahrp* (PlasmoDB ID PF3D7_0202000) locus on *P. falciparum* Chromosome 2 as an initial target. This gene is involved in the formation of ‘knobby’ projections on the surface of *P. falciparum*-infected red blood cells, and its disruption produces infected red blood cells that have a ‘smooth’ surface phenotype¹. For experimental ease and generalizability with which new loci can be targeted, we constructed two base plasmids (Fig. 2a). The first (pCas9-sgRNA-T) delivers Cas9 and the sgRNA-T targeting a specified locus. The second (pT7 RNAP-HR) delivers T7 RNAP and encodes a homologous region to repair the Cas9-sgRNA-T-induced DNA double strand break. We designed the homologous region such that successful chromosomal editing results in an in-frame transcriptional fusion of a T2a peptide-*Renilla* luciferase coding sequence¹⁵ with the upstream target gene fragment. A stop codon is included at the end of the *Renilla* gene to terminate translation. Thus, successful editing is expected to result in *Renilla* luciferase expression if the targeted gene’s promoter is transcriptionally active. We initially created three versions of pCas9-sgRNA-T from which either no sgRNA (pCas9-No sgRNA-T), pUC19-sgRNA-T (pCas9-pUC19 sgRNA-T) or *kahrp*-sgRNA-T (pCas9-*kahrp* sgRNA-T) is expressed. We separately co-transfected these plasmids with pT7 RNAP-HR^{*kahrp*} and continuously selected for episomal retention of both over the typical period (~4–6 weeks) required for obtaining easily manipulated cultures (~1% parasitemia). We used either a 3D7^{attB} parasite line with a reference firefly luciferase gene site-specifically integrated at the *cg6* locus¹⁵ or a parental 3D7 line (knob positive) in our experiments.

We monitored *Renilla* and firefly luciferase levels periodically during the course of transfection as a simple readout of successful editing within the parasite population. On post-transfection day 33, we detected a substantial increase in relative *Renilla* to firefly luciferase signal for parasites transfected with *kahrp*-sgRNA-T, but not the control pUC19-sgRNA-T (Fig. 2b). We used PCR to analyze isolated genomic DNA to determine whether the *kahrp* gene had been disrupted by insertion of the T2a-*RL* cassette in the parasite population expressing *kahrp*-sgRNA-T, but not the pUC19-sgRNA-T. Primer pairs, p1/p2 and p3/p4, designed to detect repair upstream and downstream of the cut site, respectively, yielded diagnostic PCR products only in the case for *kahrp*-sgRNA-T, but not pUC19-sgRNA-T transfections (Fig. 2c). Next, we performed Southern blot analysis to confirm that the targeted locus had been modified as expected, and to estimate the frequency of editing within the parasite population. These data indicated that virtually the entire parasite

population transfected with *kahrp*-sgRNA-T and pT7 RNAP-HR^{*kahrp*} had been successfully edited, while in pUC19-sgRNA-T and pT7 RNAP-HR^{*kahrp*}-transfected parasites, the native *kahrp* locus remained intact (Fig. 2d). Consistent with these findings, we were unable to detect KAHRP protein expression by Western blot analysis of the *kahrp*-sgRNA-T transfected parasite population. In contrast, we readily detected KAHRP in the pUC19-sgRNA-T control parasites (Fig. 2e).

In a parallel and independent experiment, we examined editing induced by the *kahrp*-sgRNA-T compared to a no sgRNA-T control in a parental 3D7 strain. Beginning on day 20, RL levels steadily increased above background, and became elevated in parasites transfected with *kahrp*-sgRNA-T but not the No sgRNA-T control (Supplementary Fig. 2a). As before, PCR analysis revealed editing at the *kahrp* locus only in the *kahrp*-sgRNA-T transfection, and Western blot confirmed that virtually no KAHRP protein was expressed at the population level (Supplementary Fig. 2b). Additionally, using scanning electron microscopy (SEM), we confirmed that parasites transfected with the no-sgRNA control plasmid retained the ‘knobby’ phenotype associated with an intact *kahrp* gene. However, the *kahrp*-sgRNA-T-transfected parasites appeared ‘smooth’, as expected for *kahrp*-null parasites (Fig. 2f). Finally, we analyzed four clones obtained by limiting dilution from the *kahrp*-sgRNA-T transfected parasite pool by PCR and Western blot. The data confirmed that these all had their *kahrp* gene disrupted, and did not express KAHRP protein (Figs. 2g,h).

Next, we examined Cas9-mediated editing at a second, unrelated genomic locus towards establishing the broader utility of this approach in the parasite. We selected the *eba-175* gene (PlasmoDB ID PF3D7_0731500) on Chromosome 7, which encodes a parasite ligand used during invasion of red blood cells¹⁶. We constructed *eba175*-sgRNA-T expression (pCas9-*eba175* sgRNA-T) and donor (pT7 RNAP-HR^{*eba175*}) plasmids (Supplementary Fig. 3a), and transfected these as described before. To evaluate editing, we isolated genomic DNA from parasites transfected in parallel with pCas9-*eba175* sgRNA-T and pT7 RNAP-HR^{*eba175*} (test) and pCas9-pUC19 sgRNA-T and pT7 RNAP-HR^{*eba175*} (control) at ~5 weeks post-transfection. Using PCR and sequencing of the resulting products, we determined that the expected editing events upstream and downstream of the induced cut site had both occurred in the *eba175*-sgRNA-T, but not the control pUC19-sgRNA-T, expressing parasite population (Supplementary Fig. 3b–c). Through Southern blot analysis, we again confirmed that the targeted locus was modified as expected (Supplementary Fig. 3d). These data suggested that ~50% of parasites within the population had been successfully edited. To address reproducibility and consistency, we repeated transfections targeting the *eba-175* locus in biological triplicates. We again verified that only pCas9-*eba175* sgRNA-T and pT7 RNAP-HR^{*eba175*} transfections were PCR positive for integration (Supplementary Fig. 3e) at ~5 weeks post-transfection. We selected one pUC19 sgRNA-T and two *eba-175* sgRNA-T samples for Southern blot analysis. Consistent with the PCR test for integration, only the *eba-175* sgRNA^T samples showed the expected insertion. Furthermore, in agreement with our previous experiment, one sample showed ~50% and the other ~80% editing at the *eba-175* locus (Supplementary Fig. 3f). Altogether, these data support high efficiency editing of endogenous loci in *P. falciparum* using the CRISPR/Cas9 system.

The potential for unintended gene disruptions due to induced off-target strand breaks and repair by the error-prone non-homologous end joining (NHEJ) mechanism has been described in human cells^{17–20}. This has led to exploration of strategies to mitigate these undesirable outcomes^{21–23}. Therefore, we sought preliminary insight into how frequent such off-target events could be in *P. falciparum*. Notably, bioinformatics analyses have revealed that *P. falciparum* lacks canonical NHEJ components^{24, 25}. Additionally, a recent study examining chromosomal double strand breaks induced by the meganuclease I-Sce1 showed that these are very efficiently and exclusively repaired by homologous donor sequence when present. In the absence of a suitable donor, however, an NHEJ-like repair process of unknown mechanism that resulted in elimination of the I-Sce1 target site was observed²⁶. To understand how an off-target Cas9 and sgRNA-T-induced chromosomal double strand break might be processed in *P. falciparum*, we simulated such an event by expressing the *kahrp*-sgRNA-T used earlier to mediate efficient editing of the *kahrp* locus, but in the absence of a suitable homologous donor plasmid [pCas9-*kahrp* sgRNA-T and pT7 RNAP]. Control parasites expressing pUC19-sgRNA-T [pCas9-pUC19 sgRNA-T and pT7 RNAP] were transfected in parallel. In two independent experiments, we observed no gross defects in relative growth between the two parasite lines generated, as both reached working parasitemias at similar times post-transfection, and qualitatively expanded comparably thereafter. To determine whether NHEJ-like events had occurred within the *kahrp* region targeted for cleavage, we isolated total genomic DNA from the *kahrp*- and pUC19- sgRNA-T transfected lines for deep sequencing. With greater than 3×10^6 reads each from the *kahrp*- and pUC19- sgRNA-T experiments, we were unable to detect indels above the limit of detection for the MiSeq sequencing method. The MiSeq error rate is about 0.001 events per 100 bp²⁷, which leads to an expected background of ~2,000 total indels at our read length (70 bp) and depth ($\sim 3 \times 10^6$). We observed ~1,500 total indels in both test and control samples, which is indistinguishable from the expected background level for the sequencing method (Fig 3b). These data suggest that NHEJ-like events occurring at Cas9-*kahrp*-sgRNA-T-induced cleavage sites are likely to be infrequent. Presently, we do not understand why cleavage induced by Cas9-sgRNA versus I-Sce1 meganuclease in the absence of a suitable donor sequence produces different repair outcomes. However, discrepancies in how double strand breaks induced by various nuclease platforms, including zinc finger nucleases, TALENs and I-Sce1, are repaired have been described²⁸. Understanding the basis for these differences in repair is an active research area given the implications for improving genome-editing efficiency. With respect to applications in *P. falciparum*, our findings taken together with previous genome editing studies using zinc finger nucleases⁵ and I-Sce1²⁶ suggest that homologous repair events should be strongly favored during CRISPR/Cas9-mediated genome editing over potentially deleterious off-target NHEJ-like outcomes.

Altogether, we demonstrate that CRISPR/Cas9 components combined with sgRNAs produced *in situ* by T7 RNA polymerase can be used to substantially increase the efficiency and technical ease with which genes can be deleted in *P. falciparum*. Indeed, with donor plasmids of a design routinely used for double crossover-mediated knockouts, we found no PCR-detectable integration events in the absence of sgRNAs directed to two distinct loci. However, within an identical timeframe, between ~50–100% of parasites expressing sgRNAs targeting these loci were edited as expected. We show that continuously selecting

for the plasmids used to express the CRISPR/Cas9 and T7 RNA polymerase components induces editing in a sufficiently large proportion of the parasite population to facilitate directly proceeding to isolating edited clones by limiting dilution. These findings promise to substantially accelerate the process for achieving targeted gene disruptions in *P. falciparum*, as it eliminates the very protracted and cumbersome selection drug cycling protocols needed to enrich the extremely rare recombination events achieved with commonly used unassisted single- and double- crossover approaches. Therefore, the ease with which the CRISPR/Cas9-T7 RNA polymerase system can be implemented in *P. falciparum* and programmed to target virtually any gene of interest makes it a highly attractive strategy for rapidly and efficiently conducting functional genetics studies in *P. falciparum*.

Methods

Materials

Molecular Biology. All plasmids used in this study were assembled using previously described methods¹⁵. Restriction enzymes and Gibson assembly master mix were purchased from New England Biolabs. Primers used in this study are summarized in Supplementary Table 1.

Accession codes—The sequences for plasmids reported in this study are deposited in GenBank under KM099231-KM099240.

Parasite culture and transfection

P. falciparum strain 3D7 parasites were grown under 5% O₂ and 5% CO₂ in RPMI-1640 media supplemented with 5 g/L Albumax II (Life Technologies), 2 g/L sodium bicarbonate, 25 mM HEPES pH 7.4 (pH adjusted with potassium hydroxide), 1 mM hypoxanthine and 50 mg/L gentamicin. For strains containing plasmids, appropriate selection drug combinations based on the markers used were added to media as follows: 2.5 mg/L blasticidin S and/or 250 mg/L G418 (Research Products International). Single and double vector transfections were carried out by the spontaneous uptake method²⁹ using ~50 µg of maxi-prepped plasmid DNA, and 8 square wave electroporation pulses of 365 V for 1 ms each, separated by 0.1 seconds. Drug selection was initiated 4 days post transfection.

Assessing T7 RNAP expression in *P. falciparum*

3D7 parasites were transfected with either pT7 RNAP (expresses T7 RNAP) or pfGNr (no T7 RNAP expression) plasmids and episomal lines selected using G418. In pT7 RNAP, T7 RNAP is expressed using the *PcDT* 5'- and *Pfhrp2* 3'- UTR pair, and selection with G418 is facilitated by *gfp-nptII* expressed from the *PfCam* 5'- and *Pfhsp86* 3'- UTR pair. To establish production of T7 RNAP protein, schizont stage parasite infected red blood cells transfected with either pT7 RNAP or pfGNr were saponin-lysed, and the lysate components separated by SDS-PAGE. Western blot analysis was carried out using a mouse anti-T7 RNAP monoclonal primary antibody (Novagen) at a 1:5,000 dilution in Tris-buffered saline, 0.1% Tween 20 and 5% milk, and an HRP-conjugated goat anti-mouse secondary antibody (Novagen) at a 1:5,000 dilution. Blots were developed using the SuperSignal West Femto kit (Pierce).

Assessing T7 RNAP activity in *P. falciparum*

To assess T7 RNAP enzymatic activity, 3D7 parasites were co-transfected with pairs of either pT7 RNAP or pfGNr and pT7 RL1, pT7 RL2 and p T7 as indicated in the text. The pT7 RL1, pT7 RL2 and p T7 plasmids encode: (i) a Blasticidin S deaminase (*bsd*) selection marker controlled by the *PfCam 5'*- and *Pfhsp86 3'*- UTR pair; and (ii) a firefly luciferase gene controlled by the *PcDT 5'* and *Pfhrp2 3'*- UTR pair. The latter is used to monitor the progress of transfections. After episomal lines were selected, total RNA for quantitative RT-PCR and Northern blot analysis was isolated from saponin-lysed schizont stage parasites. Pellets were stored in liquid nitrogen pending RNA extraction. RNA was extracted using Trizol (Life Technologies) and further purified using RNeasy purification kits (Qiagen).

For quantitative real time PCR, extracted RNA was treated with Turbo DNA-free kit (Ambion) and reverse transcribed to cDNA using the SuperScript III First Strand Synthesis System (Invitrogen). cDNA was quantified using gene specific primers (Supplementary Table 1) and SYBR Green on a LightCycler 480 Instrument II (Roche Applied Science). The thermocycling program used was as follows: Initial denaturation at 95°C for 5 min; followed by 45 cycles of 95°C for 30 s, 60°C for 30 s, and 72°C for 30s; followed by a melting curve analysis. cDNA levels were quantified relative to standard curves generated using authentic plasmid templates.

Northern blot analysis was performed using the TurboBlotter Transfer System (Whatman), and the North2South Chemiluminescent Detection kit (Thermo Scientific) for development. Authentic RNA standards were synthesized by *in vitro* transcription using the MEGAscript T7 Transcription kit (Ambion).

Quantitative growth assays

Relative growth rates for the following dual transfected parasite lines were determined: (1) pfGNr (No T7 RNAP) and p T7 (No T7 promoter-driven cassette); (2) pfGNr and pT7 RL1; (3) pT7 RNAP and p T7; and (4) pT7 RNAP and pT7 RL1. Synchronized ring stage parasites were set up in triplicate in 96-well microtiter plates and seeded at < 2% parasitemia and 2% hematocrit in 200 μ l media containing both G418 and Blasticidin S. The p T7 plasmid, which confers Blasticidin S resistance, was used in the no pT7 RL1 co-transfections, while the pfGNr plasmid, which confers G418 resistance but does not express T7 RNAP, was used in the no T7 RNAP expression conditions. This permitted co-selection of all test lines with G418 and Blasticidin S to eliminate this as a variable in the outcomes of the growth assays. Expansion was measured over four generations at the trophozoite stage. At each measurement, cultures were split to achieve an initial parasitemia < 2% to avoid over-expansion. Parasitemias were measured by fixing for 3 hours in 1% formaldehyde acid citrate dextrose (ACD) buffer prior to SYBR Green I staining and analysis by flow cytometry (Accuri C6). Expansion rates were normalized to the control line (pfGNr and p T7, identified as '- pT7 RL1, - pT7 RNAP' in Fig. 1f) for each time point measured.

In vitro Cas9 cleavage assays

In vitro cleavage assays were performed as previously described³⁰. Briefly, HEK 293FT cells were transfected with the Cas9 expression plasmid pX165⁹ in 6-well plates using

Lipofectamine 2000 (Life Technologies) according to the manufacturer's protocol. Forty eight hours post-transfection, cells were lysed with 250 μ l Lysis Buffer (20 mM HEPES pH 7.5, 100 mM potassium chloride, 5 mM magnesium chloride, 1 mM dithiothreitol, 5% glycerol, 0.1% Triton X-100) supplemented with a protease inhibitor cocktail (Roche). Lysates were sonicated for 10 minutes and cell debris pelleted by centrifugation for 20 min at 5,000 x *g*. Lysates containing Cas9 protein were aliquoted and stored at -80°C .

sgRNA-Ts were *in vitro* transcribed using the MEGAscript T7 kit (Ambion) using a circular plasmid template containing a cassette for T7 RNAP dependent expression of the specific sgRNA as a template. The target DNA was amplified from *P. falciparum* genomic DNA with primers specific to the gene being tested (Supplementary Table 1).

CRISPR/Cas9 genome editing in *P. falciparum*

Plasmids encoding either T7 RNAP with homologous donor regions (pT7 RNAP-HR) or not (pT7 RNAP) and Cas9 with a sgRNA (pCas9-sgRNA-T) or not (pCas9-No sgRNA-T) were co-transfected as indicated into 3D7 and 3D7^{attB}::FLuc¹⁵ (*kahrp* locus targeted) or NF54^{attB}³¹ (*eba-175* locus targeted) backgrounds. Cas9 and *bsd* selection marker expression are controlled by the *PcDT* 5'- and *Pfhrp2* 3'- and *PfCam* 5'- and *Pfhsr86* 3'- UTR pairs, respectively. In negative control experiments, either no sgRNA or one targeting a region in the ampicillin resistance gene on the pUC19 plasmid and that is not present in the *P. falciparum* genome were used. Approximately 50 μ g of each plasmid were co-transfected and simultaneously selected beginning at four days post transfection. Luciferase levels were measured periodically to determine if genomic editing had occurred during experiments when the *kahrp* gene was targeted. Parasites were detectable by Giemsa smear within a typical 4–6 week transfection period. The analyses reported here were done over the ensuing several weeks thereafter. Main cultures were kept under drug selection, while no drug pressure was applied during clone isolation.

Analysis of CRISPR-edited parasite lines

Firefly and *Renilla* luciferase levels were measured using the Dual-Luciferase Reporter Assay System (Promega). Infected red blood cells were lysed using passive lysis buffer supplied with the kit, and measurements made according to the manufacturer's instructions on a Glomax 20/20 luminometer (Turner Biosystems).

PCR analyses to assess modification of the targeted loci were carried out using a 15:1 (v:v) mixture of Hemo KlenTaq:Pfu Turbo (Agilent) in Hemo KlenTaq Buffer with genomic DNA purified from saponin-lysed cultures using the QIAamp DNA blood mini kit (Qiagen). The primers used are included in Supplementary Table 1.

Samples for KAHRP western blot analysis were obtained by repeated hypotonic lysis of infected red blood cells in water, followed by high-speed centrifugation (21,000 x *g* for 1 min). The membrane fraction was recovered, solubilized in 1x SDS loading buffer, and separated by SDS-PAGE. For KAHRP detection, a primary mouse monoclonal anti-KAHRP antibody (mAb 89) provided by Diane Taylor was used at a 1:1,000 dilution in combination with a secondary HRP-conjugated goat anti-mouse secondary antibody (Novagen) at a

1:5,000 dilution. Blots were developed using the SuperSignal West Femto kit (Pierce). For NPTII detection, blots were probed with anti-NPTII antibody (Millipore 06–747) at a 1:1,000 dilution, and developed with secondary as described above.

Southern blots were carried out on DNA purified from infected red blood cells using the QIAamp DNA blood mini kit (Qiagen) after saponin lysis. Samples were restriction enzyme digested overnight with HindIII, BamHI and PstI, and HindIII and XbaI for analysis of the *kahrp* and *eba-175* loci, respectively. Blots were processed using the TurboBlotter kit (Whatman) for transfer, and the North2South kit (Thermo Scientific) for development.

Scanning electron microscopy (SEM) was performed as described³² on a JEOL 5600LV SEM instrument operated at 10 kV.

Deep sequencing

We performed deep sequencing as previously described²². Briefly, the target site within the *kahrp* gene was amplified by PCR to include generic handles. Using the handles as priming sequences, a second round of PCR was performed to include unique barcodes for sample identification as well as Illumina P5 and P7 adapters. PCR products were pooled in an equimolar ratio and purified by the QIAquick Gel Extraction Kit (Qiagen). Barcoded and purified pooled sequencing libraries were quantified using the Qubit dsDNA HS Assay Kit (Life Technologies) and sequenced using the Illumina MiSeq Personal Sequencer (Life Technologies).

Supplementary Material

Refer to Web version on PubMed Central for supplementary material.

Acknowledgments

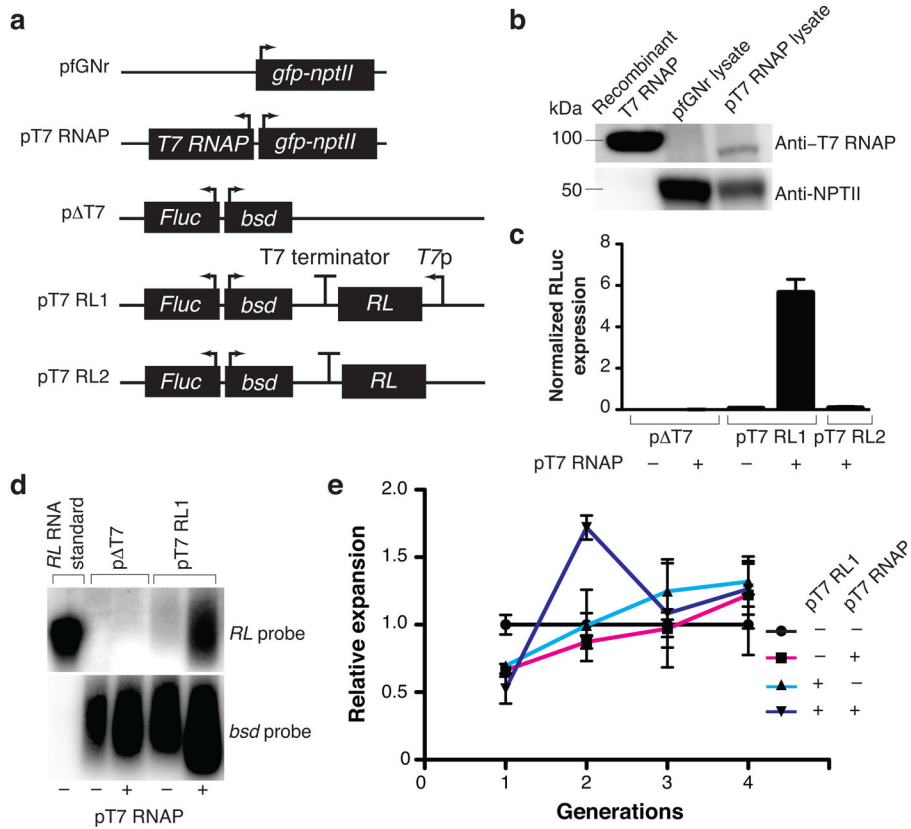
We thank D. Taylor (University of Hawaii) for providing the anti-KAHRP mAb 89 antibody used for western blots and N. Watson (W. M. Keck Microscopy Facility at the Whitehead Institute) for technical assistance with SEM imaging. The following reagent was obtained through the MR4 as part of the BEI Resources Repository, NIAID, NIH: *Plasmodium falciparum* pfGNr malaria expression vector, MRA-462, deposited by C. Plowe. Quantitative PCR analyses were performed through the Genomics and Imaging Facilities Core of the MIT Center for Environmental and Health Sciences, which is supported by NIEHS Center Grant P30-ES002109. This work was supported by NIGMS Biotechnology Training Grant 5-T32-GM08334 (J.C. Wagner) and NIEHS Training Grant in Toxicology 5-T32-ES007020 (S.J. Goldfless). This material is based upon work supported by the National Science Foundation Graduate Research Fellowship under Grant No. 1122374 (R.J. Platt), an NIH Director's New Innovator Award (1DP2OD007124) to J.C. Niles, and funded by a grant from the Bill and Melinda Gates Foundation through the Grand Challenges Explorations initiative (OPP1069759) to J.C. Niles.

References

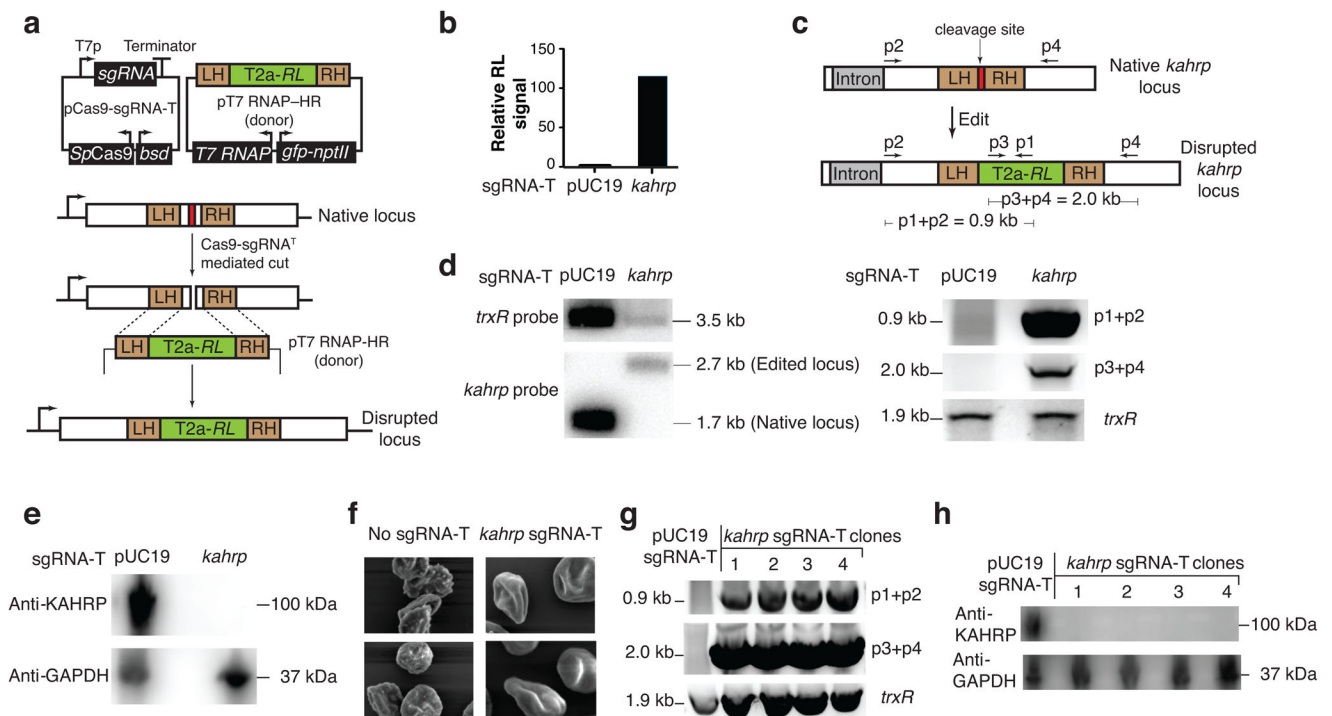
1. Crabb BS, et al. Targeted gene disruption shows that knobs enable malaria-infected red cells to cytoadhere under physiological shear stress. *Cell*. 1997; 89:287–296. [PubMed: 9108483]
2. Crabb BS, Cowman AF. Characterization of promoters and stable transfection by homologous and nonhomologous recombination in *Plasmodium falciparum*. *Proceedings of the National Academy of Sciences of the United States of America*. 1996; 93:7289–7294. [PubMed: 8692985]
3. Wu Y, Kirkman LA, Welles TE. Transformation of *Plasmodium falciparum* malaria parasites by homologous integration of plasmids that confer resistance to pyrimethamine. *Proceedings of the National Academy of Sciences of the United States of America*. 1996; 93:1130–1134. [PubMed: 8577727]

4. Crabb BS, et al. Transfection of the human malaria parasite *Plasmodium falciparum*. *Methods in Molecular Biology* (Clifton, NJ). 2004; 270:263–276.
5. Straimer J, et al. Site-specific genome editing in *Plasmodium falciparum* using engineered zinc-finger nucleases. *Nature Methods*. 2012; 9:993–998. [PubMed: 22922501]
6. Maeder ML, Thibodeau-Beganny S, Sander JD, Voytas DF, Joung JK. Oligomerized pool engineering (OPEN): an ‘open-source’ protocol for making customized zinc-finger arrays. *Nature Protocols*. 2009; 4:1471–1501.
7. Sander JD, et al. Selection-free zinc-finger-nuclease engineering by context-dependent assembly (CoDA). *Nature Methods*. 2011; 8:67–69. [PubMed: 21151135]
8. Bassett AR, Tibbit C, Ponting CP, Liu JL. Highly efficient targeted mutagenesis of *Drosophila* with the CRISPR/Cas9 system. *Cell Reports*. 2013; 4:220–228. [PubMed: 23827738]
9. Cong L, et al. Multiplex genome engineering using CRISPR/Cas systems. *Science (New York, NY)*. 2013; 339:819–823.
10. Dickinson DJ, Ward JD, Reiner DJ, Goldstein B. Engineering the *Caenorhabditis elegans* genome using Cas9-triggered homologous recombination. *Nature Methods*. 2013; 10:1028–1034. [PubMed: 23995389]
11. Hwang WY, et al. Efficient genome editing in zebrafish using a CRISPR-Cas system. *Nature Biotechnology*. 2013; 31:227–229.
12. Mali P, et al. RNA-guided human genome engineering via Cas9. *Science (New York, NY)*. 2013; 339:823–826.
13. Russell K, Hasenkamp S, Emes R, Horrocks P. Analysis of the spatial and temporal arrangement of transcripts over intergenic regions in the human malarial parasite *Plasmodium falciparum*. *BMC Genomics*. 2013; 14:267. [PubMed: 23601558]
14. Wakaguri H, et al. Full-Malaria/Parasites and Full-Arthropods: databases of full-length cDNAs of parasites and arthropods, update 2009. *Nucleic Acids Research*. 2009; 37:D520–525. [PubMed: 18987005]
15. Wagner JC, et al. An integrated strategy for efficient vector construction and multi-gene expression in *Plasmodium falciparum*. *Malaria Journal*. 2013; 12:373. [PubMed: 24160265]
16. Reed MB, et al. Targeted disruption of an erythrocyte binding antigen in *Plasmodium falciparum* is associated with a switch toward a sialic acid-independent pathway of invasion. *Proceedings of the National Academy of Sciences of the United States of America*. 2000; 97:7509–7514. [PubMed: 10861015]
17. Cho SW, et al. Analysis of off-target effects of CRISPR/Cas-derived RNA-guided endonucleases and nickases. *Genome Research*. 2014; 24:132–141. [PubMed: 24253446]
18. Cradick TJ, Fine EJ, Antico CJ, Bao G. CRISPR/Cas9 systems targeting beta-globin and CCR5 genes have substantial off-target activity. *Nucleic Acids Research*. 2013; 41:9584–9592. [PubMed: 23939622]
19. Fu Y, et al. High-frequency off-target mutagenesis induced by CRISPR-Cas nucleases in human cells. *Nature Biotechnology*. 2013; 31:822–826.
20. Pattanayak V, et al. High-throughput profiling of off-target DNA cleavage reveals RNA-programmed Cas9 nuclease specificity. *Nature Biotechnology*. 2013; 31:839–843.
21. Fu Y, Sander JD, Reyon D, Cascio VM, Joung JK. Improving CRISPR-Cas nuclease specificity using truncated guide RNAs. *Nature Biotechnology*. 2014
22. Hsu PD, et al. DNA targeting specificity of RNA-guided Cas9 nucleases. *Nature Biotechnology*. 2013; 31:827–832.
23. Ran FA, et al. Double nicking by RNA-guided CRISPR Cas9 for enhanced genome editing specificity. *Cell*. 2013; 154:1380–1389. [PubMed: 23992846]
24. Aravind L, Iyer LM, Wellems TE, Miller LH. *Plasmodium* biology: genomic gleanings. *Cell*. 2003; 115:771–785. [PubMed: 14697197]
25. Gardner MJ, et al. Genome sequence of the human malaria parasite *Plasmodium falciparum*. *Nature*. 2002; 419:498–511. [PubMed: 12368864]

26. Kirkman LA, Lawrence EA, Deitsch KW. Malaria parasites utilize both homologous recombination and alternative end joining pathways to maintain genome integrity. *Nucleic Acids Research*. 2014; 42:370–379. [PubMed: 24089143]
27. Junemann S, et al. Updating benchtop sequencing performance comparison. *Nature Biotechnology*. 2013; 31:294–296.
28. Kuhar R, et al. Novel fluorescent genome editing reporters for monitoring DNA repair pathway utilization at endonuclease-induced breaks. *Nucleic Acids Research*. 2014; 42:e4. [PubMed: 24121685]
29. Deitsch K, Driskill C, Wellems T. Transformation of malaria parasites by the spontaneous uptake and expression of DNA from human erythrocytes. *Nucleic Acids Research*. 2001; 29:850–853. [PubMed: 11160909]
30. Jinek M, et al. RNA-programmed genome editing in human cells. *eLife*. 2013; 2:e00471. [PubMed: 23386978]
31. Adjalley SH, et al. Quantitative assessment of *Plasmodium falciparum* sexual development reveals potent transmission-blocking activity by methylene blue. *Proceedings of the National Academy of Sciences of the United States of America*. 2011; 108:E1214–1223. [PubMed: 22042867]
32. Rug M, Prescott SW, Fernandez KM, Cooke BM, Cowman AF. The role of KAHRP domains in knob formation and cytoadherence of *P. falciparum*-infected human erythrocytes. *Blood*. 2006; 108:370–378. [PubMed: 16507777]

**Figure 1.**

Validating T7 RNA polymerase functions in *P. falciparum*. **(a)** Schematic of the Cas9, sgRNA and target DNA interaction. The sgRNA base pairs with a 20 nucleotide target DNA region defined by an NGG protospacer adjacent motif (PAM). Cas9 induces double strand DNA cleavage (arrow heads) 3 nucleotides upstream of the PAM site. **(b)** Plasmids used to test T7 RNAP expression and activity. In the reporter plasmid, pT7 RL1, the *Renilla* luciferase (*RL*) gene is expressed from a T7 promoter-T7 terminator cassette. The pT7 RL2 control plasmid contains the RL gene and T7 terminator, but no T7 promoter. A second control plasmid, p T7, lacks the T7 promoter-RL gene-T7 terminator cassette. **(c)** Western blot analysis of T7 RNAP protein production in parasites. Blots were probed with anti-T7 RNAP and anti-NPTII (loading control) antibodies. **(d)** Quantitative RT-PCR analysis of normalized *RL* transcript levels produced after the indicated transfections. Levels are above background only for the pT7 RNAP plus pT7 RL1 case. Data shown are mean \pm s.d. (n = 3 technical replicates). **(e)** Northern blot analysis for *RL* transcript production, with the *bsd* selection marker transcript probed as a control. **(f)** Relative parasite growth over four successive generations both in the presence or absence of T7 RNAP and a T7 promoter-driven expression cassette. Data are shown as mean \pm s.d. (n = 3 biological replicates) and analyzed for significance by One-way ANOVA.

**Figure 2.**

CRISPR/Cas9-mediated disruption of the *P. falciparum* *kahrp* locus. **(a)** Generalized schematic of the Cas9 and T7 promoter-driven sgRNA-T plasmid used for genome editing. For homology directed repair of the induced double strand break, pT7 RNAP is modified to include homologous regions flanking a T2a-RL gene. Successful repair eliminates the original sgRNA target site, and creates a translational fusion between the upstream fragment of the disrupted target and the T2a-RL genes. **(b)** Measurement of RL expression in parasite population when the *kahrp* locus is targeted by a *kahrp*-sgRNA-T or pUC19-sgRNA-T control in the presence of a suitable donor plasmid. **(c)** PCR primers to specifically detect homology-directed repair at a target cut site in the *kahrp* locus amplify products of the expected size for *kahrp*-sgRNA-T but not pUC19-sgRNA-T transfected parasite population. **(d)** Southern and **(e)** Western blot analyses of parasite populations obtained after transfection with the pUC19- and *kahrp*- sgRNA-Ts. **(f)** SEM imaging analysis of parasite populations obtained after transfection with a no sgRNA-T control and a *kahrp*- sgRNA-T. **(g, h)** PCR and Western blot analyses as in **(c)** and **(e)**, respectively, of cloned parasites derived from the *kahrp*-sgRNA-T edited pool. The unedited pUC19-sgRNA-T pool with an intact native *kahrp* locus is used as a positive control.

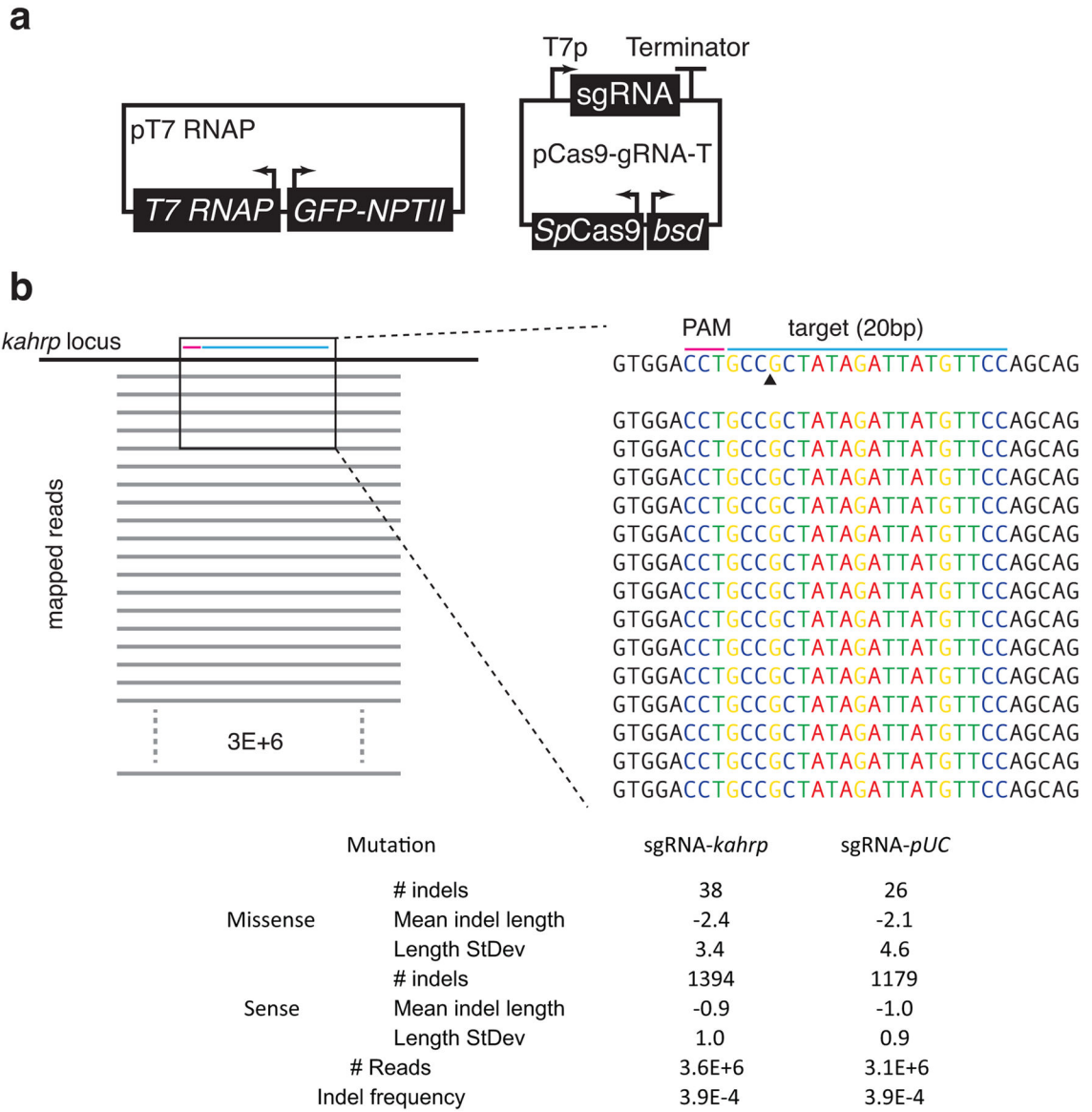


Figure 3. Assessing the fate of *kahrp*-sgRNA-T-induced cleavage of the *kahrp* locus in the absence of a homologous donor plasmid. **(a)** Schematic of the validated pT7 RNAP and pCas9-*kahrp* sgRNA-T plasmids used in this experiment. **(b)** Deep sequencing analysis of the region targeted for cleavage by *kahrp*-sgRNA-T. A representative set (1 of 3 independent experiments) of twenty bacterial clones analyzed by Sanger sequencing is illustrated.